Properties of the Glucose-6-Phosphate Transporter from *Chlamydia pneumoniae* (HPTcp) and the Glucose-6-Phosphate Sensor from *Escherichia coli* (UhpC)†

Christian Schwöppe,[1] Herbert H. Winkler,[2] and H. Ekkehard Neuhaus[1]*

Pflanzenphysiologie, Universität Kaiserslautern, D-67653 Kaiserslautern, Germany,[1] and Department of Microbiology and Immunology, College of Medicine, University of South Alabama, Mobile, Alabama 36688[2]

The amino acid sequence of the proposed glucose-6-phosphate (Glc6P) transporter from *Chlamydia pneumoniae* (HPTcp; hexose phosphate transporter [*Chlamydia pneumoniae*]) exhibits a higher degree of similarity to the *Escherichia coli* Glc6P sensor (UhpC) than to the *E. coli* Glc6P transporter (UhpT). Overexpression of His-UhpC in a UhpT-deficient *E. coli* strain revealed that the sensor protein is also able to transport Glc6P and exhibits an apparent $K_{m\,(Glc6P)}$ of 25 µM, whereas His-HPTcp exhibits an apparent $K_{m\,(Glc6P)}$ of 98 µM. His-HPTcp showed a four-times-lower specific activity than His-UhpT but a 56-times-higher specific activity than His-UhpC. Like His-UhpT and His-UhpC, the carrier His-HPTcp performs a sugar-phosphate/inorganic-phosphate antiporter mode of transport. Surprisingly, while physiological concentrations of inorganic phosphate competitively inhibited transport mediated by the *E. coli* proteins His-UhpT and His-UhpC, transport mediated by His-HPTcp was not inhibited. Interestingly, C_3-organophosphates stimulated His-HPTcp activity but not His-UhpT- or His-UhpC-catalyzed Glc6P transport. In contrast to His-UhpC, the His-HPTcp protein does not act as a Glc6P sensor in the *uhp* regulon.

Escherichia coli transports glucose-6-phosphate (Glc6P) via an inducible transport protein named UhpT that is part of the genomic locus *uhp* which encodes UhpT (the Glc6P transport protein), UhpB (the membrane-bound sensor kinase/phosphatase), UhpA (a soluble signal transduction component) and UhpC (the sensor for the presence of extracellular Glc6P) (15). UhpT is a typical member of the major facilitator superfamily (MFS) that is predicted to have 12 α-helical transmembrane domains (17). The amino acid sequence of the *E. coli* UhpC protein exhibits 32% identity to the transport protein UhpT and both proteins share the same predicted transmembrane topology (15). It is proposed that upon recognition of extracellular Glc6P UhpC induces auto-phosphorylation of UhpB. Subsequent to this, UhpB~P transfers its phosphate group to the soluble component UhpA, which then gains activity as a transcription activator governing the expression of the structural *uhpT* gene (27).

In former times, the analysis of the functional presence of UhpT-like proteins in other bacterial species usually depended upon the demonstration of inorganic phosphate (P_i)-linked hexose phosphate uptake. Using this approach, Glc6P transport has also been identified, for example, in *Streptococcus lactis* (2) and *Salmonella enterica* serovar Typhimurium (14). Also, sensitivity to fosfomycin, an antibiotic compound that enters the bacterial cell via the GlcT or the UhpT protein, was surveyed in several bacterial species to determine how widespread hexose phosphate transport is (26). Today, the completed sequences of more than 50 bacterial genomes that allow insights into the presence or absence of certain proteins are available.

The genomes of the human-pathogenic bacteria *Chlamydia trachomatis* and *Chlamydia pneumoniae* contain a structural gene coding for a protein with high identity to the *E. coli* Glc6P transporter (23). A more detailed analysis revealed that the deduced amino acid sequences of the chlamydial proteins exhibit a higher degree of identity to the *E. coli* Glc6P sensor UhpC (45% identity) than to the transport protein UhpT (30% identity). Because the chlamydial genome does not harbor an open reading frame coding for hexokinase, a glucose group translocation/phosphotransferase system or genes encoding proteins with homology to other elements of the *uhp* regulon (e.g., uhpT, uhpA, and uhpB) (23), it seemed likely that the chlamydial protein (named HPTcp; hexose phosphate transporter [*C. pneumoniae*]) functions as a Glc6P transporter and not as a sensor.

Such an evolutionary relationship suggests that *E. coli* UhpC may function not only as a sensor but also as a Glc6P transporter. Although it has previously been speculated that transport of Glc6P by UhpC is not necessary to induce the expression of *uhpT* (15), it is of general biological interest to verify whether UhpC is able to transport Glc6P (as we claim for HPTcp) and to characterize its basic biochemical properties. Moreover, from the point of view of human infections caused by various chlamydial species it is of interest to study the biochemical properties of transport proteins involved in the metabolism of the intracellular pathogen.

Therefore, we addressed the following questions. (i) Is the *E. coli* Glc6P sensor UhpC also able to transport Glc6P? (ii) If so, what are the basic transport properties of UhpC? (iii) Is HPTcp a Glc6P transport protein and do the basic biochemical

* Corresponding author. Mailing address: Universität Kaiserslautern, Pflanzenphysiologie, Postfach 3049, D-67653 Kaiserslautern, Germany. Phone: 0631/205-2372. Fax: 0631/205-2600. E-mail: Neuhaus@rhrk.uni-kl.de.

properties of this carrier support the idea that the chlamydial *hptcp* gene entered the genome via horizontal transfer of a UhpC module? (iv) Finally, is HPTcp able to act as a Glc6P sensor in the *E. coli uhp* regulon?

MATERIALS AND METHODS

DNA constructs for heterologous expression in *E. coli*. DNA manipulations were performed essentially as described previously (21). The structural genes encoding UhpC and UhpT, respectively, were amplified from the genomic DNA of *E. coli* XL1-Blue. The structural gene encoding HPTcp was amplified from the genomic DNA of *C. pneumoniae* (kindly provided by G. McClarty, University of Manitoba, Winnipeg, Manitoba, Canada). PCR was carried out by using *Pfu* DNA polymerase (Stratagene, Heidelberg, Germany). The primers used were constructed according to infomation taken from the *E. coli* and the *C. pneumoniae* genome projects. The sense primers (*uhp*C, 5′-CTAAGGTTTGCATA TGTTGCCGTTTCTG-3′; *uhp*T, 5′-CAGGAGTAACATATGCTGGCTTTCT TAAAC-3′; and *hptcp*, 5′-GGAAATTGACATATGAACGTTTGGACT-3′) contained a *Nde*I restriction site at the start codon, whereas the antisense primers (*uhp*C, 5′-AAAGCTGAGATGCATCACGCTTCG-3′; *uhp*T, 5′-GCCGGG CAAAAGGATCCAGTTTCGTTTATG-3′; and *hptcp*, 5′-AACGGCTAGGCT TTACTACG-3′) contained the stop codon for the corresponding sequence. The PCR products were gel purified, cloned into the *Eco*RV site of plasmid pBSK (Stratagene), and sequenced on both strands by chain termination reaction (Seqlab, Göttingen, Germany). To construct plasmids expressing an N-terminal histidine tag, the *Nde*I/*Bam*HI DNA inserts of the pBSK constructs were introduced into the *Nde*I/*Bam*HI sites of the bacterial vector pET16b (Novagen, Heidelberg, Germany).

Recently, it has been shown that the *E. coli* expression plasmid pT7-5 allows higher yields of heterologously expressed membrane proteins (1). Therefore, we used this plasmid as a suitable tool to overexpress the histidine-tagged transporter proteins. PCRs were carried out by using the *uhp*C/pET16b and *hptcp*/ pET16b constructs as templates. For this, the sense primer OL30 (5′-GAACG GATCCATACCATGGGC-3′) and the T7-terminator primer were used, leading to the introduction of a *Bam*HI restriction site at the 5′ end. The resulting PCR products were gel purified, subsequently cut with *Bam*HI, and introduced into the *Bam*HI-digested vector pMA618 (a pT7-5 derivate). After the correct orientation was analyzed, these constructs were used for overexpression of His-UhpC and His-HPTcp in *E. coli*.

Strains, P1 transduction and growth conditions. Strain XL1-Blue (Stratagene) was used for all cloning steps. Strains RK7245 [*uhp*C::Tn*1000* (Tet^r)] and RK7251 [*uhp*T::Tn*1000* (Tet^r); kindly provided by Robert Kadner, University of Virginia, Charlottesville] were used as donor strains for P1 transduction of *E. coli* BL21(DE3) to create UhpC- and UhpT-deficient BL21(DE3) mutants. This *E. coli* strain was chosen to receive an appropriate inducible system for uptake experiments with intact bacterial cells. P1 transduction was carried out with P1 *vir* essentially as described previously (3). Subsequently, the plasmids pET16b (control), *uhp*C/pET16b, *hptcp*/pET16b, and *uhp*T/pET16b were introduced into the UhpC- and UhpT-deficient *E. coli* strain BL21(DE3) (*uhp*C::Tn*1000* and *uhp*T::Tn*1000*, respectively). Transformation of *E. coli* was carried out according to standard protocols.

Overnight cultures were diluted 100-fold into YT medium plus antibiotics and grown at 37°C to an optical density (A_{578}) of 0.5 to 0.6. Induction of T7-RNA polymerase was initiated by addition of IPTG (final concentration, 0.012%). Cells were grown for an additional 90 min, collected by centrifugation, resuspended in morpholinepropanesulfonic acid (MOPS) and buffer medium (50 mM, pH 7.5), and stored on ice until use.

As the heterologous host strain for the purification of histidine-tagged membrane proteins by metal-affinity chromatography, we used *E. coli* BL21(DE3) C43 (kindly provided by John E. Walker, University of Cambridge, Cambridge, United Kingdom) with Terrific Broth (11) as growth medium.

For assays of P$_i$ transport cells were grown in M63 minimal medium (pH 7.5) (10) containing thiamine (2 μg/ml), Casamino Acids (50 μg/ml), necessary antibiotics, and 0.2% (wt/vol) glucose. Cultures were grown overnight and induced with IPTG (isopropyl-β-D-thiogalactopyranoside). After an additional 2 h the cells were harvested by centrifugation and washed twice with MOPS buffer medium.

Transport assays. Cell suspensions were allowed to equilibrate at 30°C and subsequently mixed with the same amount of prewarmed transport medium containing [^{14}C]Glc6P (NEN, Frankfurt/Main, Germany). At the indicated time points transport was stopped by transfer of cells to membrane filters (25 mm in diameter, 0.45-μm pore size; Orange Scientific, Braine-l'Alleud, Belgium)

prewetted with MOPS buffer medium and set under a vacuum. After being washed with buffer, the filters were placed in vials containing scintillation cocktail (Quicksafe A; Zinsser Analytic, Frankfurt/Main, Germany). For P$_i$ efflux assays the washed cells were first incubated with 100 μM ^{32}P$_i$ (NEN). Subsequently, they either received unlabeled KP$_i$ (final concentration, 10 mM) or they were washed twice with MOPS buffer medium and resuspended in buffer containing the indicated counter-exchange substrate. The transport was stopped as described above, and the filters were transferred into vials containing water. Radioactivity was quantified in a Canberra-Packard Tricarb-2500 Counter (Canberra-Packard, Frankfurt/Main, Germany).

The kinetic constants of transport were estimated by the method of Hanes. Inhibition constants (K_i) for P$_i$ were determined by using the Dixon plot analysis. All data represent the means of at least three independent experiments. The standard deviation was always less than 8% of the given mean. The background activity of IPTG-induced *E. coli* cells (*uhp*T::Tn*1000*) harboring the vector plasmid pET16b was subtracted. The protein content of *E. coli* samples was quantified by using Coomassie brilliant blue according to the method of Bradford (4).

Cytoplasmic membrane preparation, purification of histidine-tagged membrane protein, and Western blot analysis. Cytoplasmic membrane preparation and purification of histidine-tagged membrane protein were carried out as described before (1). The cells were disrupted by ultrasonication (250 W, three times for 30 s each time, 4°C). The membrane proteins were solubilized by the addition of *n*-dodecyl maltoside and purified by Ni-chelating chromatography according to supplier′s instructions (Qiagen, Hilden, Germany). To increase the amounts of membrane protein for the purification procedure of the histidine-tagged proteins, *E. coli* C43 harboring the IPTG-inducible pMA618 construct of His-UhpC or His-HPTcp, respectively, was used (see above). The resulting membrane protein fractions were separated by sodium dodecyl sulfate-polyacrylamide gel electrophoresis.

For Western blot analysis, *E. coli* BL21(DE3) (*uhp*T::Tn*1000*) harboring the corresponding pET16b construct was used as described above for the transport assays. Cytoplasmic membrane preparation was carried out as described previously (1). Western blots were developed by using a histidine-tag specific antiserum (Qiagen, Hilden, Germany) and the method of chemiluminescence (Roche, Mannheim, Germany). Expression levels were determined by densitometry of digitized images (9). The linearity of densitometry was checked by applying various amounts of protein.

RESULTS

Structural characteristics of UhpC and HPTcp. The genome from *C. pneumoniae* contains the gene *hptcp* encoding a highly hydrophobic protein of 455 amino acid residues exhibiting 30% identity to the Glc6P transporter UhpT from *E. coli*. Because of this high degree of similarity it is not surprising that the chlamydial protein possesses, like UhpT, 12 predicted transmembrane domains. An amino acid alignment revealed that conserved amino acids are scattered throughout the entire HPTcp protein in hydrophilic as well as in predicted transmembrane regions. However, the lowest conservation between these proteins is present in the large hydrophilic loop connecting transmembrane domains 6 and 7 (data not shown).

UhpC has already been identified as a protein with substantial structural similarities to the *E. coli* Glc6P transporter UhpT (15). Interestingly, the chlamydial HPTcp protein exhibits 45% identity to the Glc6P sensor protein UhpC, which is significantly higher than that to the Glc6P transporter UhpT (see above).

Glc6P transport into *E. coli* catalyzed by His-UhpC or His-HPTcp. To analyze whether UhpC (analyzed as a His-UhpC protein) is able to transport Glc6P, we used an *E. coli* BL21 (DE3) mutant lacking a functional UhpT protein (*uhp*T:: Tn*1000*). After transformation of these cells with the plasmid *uhp*C/pET16b and IPTG-induced expression, these *E. coli* cells were able to import Glc6P (Fig. 1A). After 1 min of incubation with radioactively labeled Glc6P, negative control cells harbor-
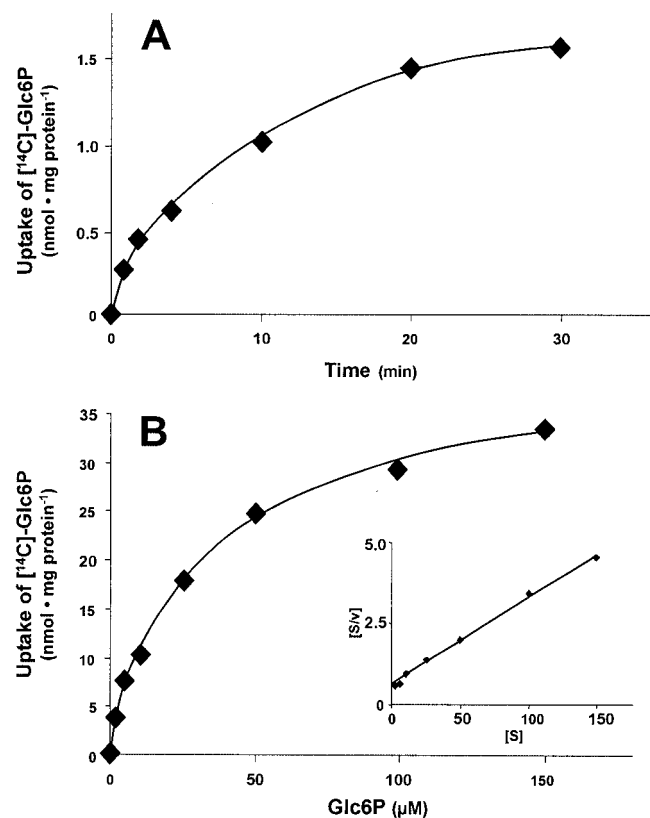
FIG. 1. Uptake of [^{14}C]Glc6P into IPTG-induced *E. coli* cells (*uhpT*::Tn*1000*) harboring plasmid *uhpC*/pET16b. (A) Time dependency of [^{14}C]Glc6P uptake (at a concentration of 25 μM). (B) Substrate saturation of [^{14}C]Glc6P uptake. Cells were incubated for 1 min with the indicated concentrations. Inset: Hanes plot of the [^{14}C]Glc6P uptake, indicating an apparent K_m of 25 μM and a V_{max} of 38 nmol per mg of protein per h.

FIG. 2. Uptake of [^{14}C]Glc6P into IPTG-induced *E. coli* cells (*uhpT*::Tn*1000*) harboring plasmid *hptcp*/pET16b. (A) Time dependency of [^{14}C]Glc6P uptake (at a concentration of 100 μM). (B) Substrate saturation of [^{14}C]Glc6P uptake. Cells were incubated for 1 min with the indicated concentrations. Inset: Hanes plot of the [^{14}C]Glc6P uptake, indicating an apparent K_m of 98 μM and a V_{max} of 200 nmol per mg of protein per h.

ing the vector pET16b imported radioactivity at a rate ca. 1/6 that of the cells harboring *uhpC*/pET16b (data not shown). The slow rate of radioactivity import observed in control cells may be due either to residual activity of the endogenous UhpC carrier or to uptake of free glucose liberated after extracellular dephosphorylation of Glc6P. We prefer the latter explanation because the addition of glucose (5 mM) totally blocked uptake of radioactivity into control cells (data not shown; in further experiments, however, we did not add glucose). Therefore, to allow a correct determination of substrate affinity and to study the action of various effectors, we always subtracted uptake of radioactivity into IPTG-induced control cells harboring the empty vector pET16b. Glc6P uptake was linear for ca. 2 min and reached the steady state after ca. 30 min of incubation. Glc6P uptake by His-UhpC exhibited an apparent affinity (K_m) of 25 μM and occurred at a maximal rate of 38 nmol per mg of *E. coli* protein per h (Fig. 1B and inset).

To elucidate the substrate transport properties of His-HPTcp, we transformed the mutated *E. coli* cells (*uhpT*::Tn*1000*) with plasmid *hptcp*/pET16b and induced expression of the transporter gene with IPTG. Glc6P uptake into *E. coli* catalyzed by His-HPTcp was linear with time for ca. 2.5 min (Fig. 2A), exhibited an apparent K_m value of 98 μM and
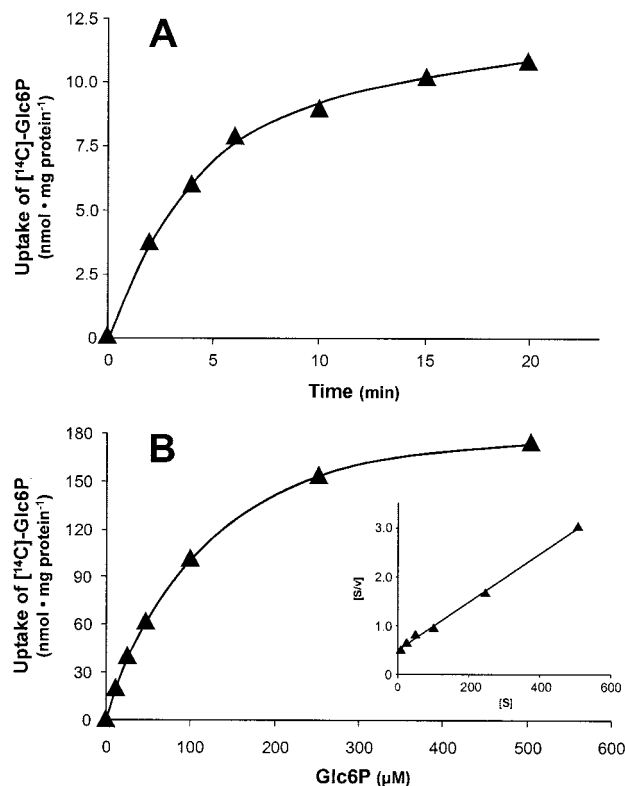
occurred at a maximal rate of 200 nmol per mg of *E. coli* protein per h (Fig. 2B and inset).

To gain insight into the specific activities of these carrier proteins, we compared the protein levels of His-UhpT, His-UhpC, and His-HPTcp in the *E. coli* cell membranes with the corresponding Glc6P uptake rates. As shown in Fig. 3A, lane 3, the metal-chelate affinity-purified His-HPTcp protein exhibits an apparent molecular mass of ca. 45 kDa, whereas the purified His-UhpC protein has a molecular mass of ca. 39 kDa. These values are substantially less than the calculated authentic molecular masses of the His-HPTcp and the His-UhpC proteins (54.1 and 50.7 kDa, respectively; His-UhpT exhibits a calculated molecular mass of 53.1 kDa). However, it is well known that hydrophobic membrane proteins tend to bind unrepresentative amounts of sodium dodecyl sulfate and thus exhibit lower apparent molecular masses.

A Western blot analysis with a histidine tag-specific antiserum allowed quantification of the relative abundance of His-UhpT, His-UhpC, and His-HPTcp in the *E. coli* membrane (Fig. 3B). Most prominent was the His-UhpC protein (Fig. 3B, lane 1). Setting the presence of His-UhpC to 100%, the His-HPTcp entered the *E. coli* membrane with 9.5% efficiency and the His-UhpT entered the *E. coli* membrane with 37% efficiency (Fig. 3B, lanes 2 and 3). The corresponding maximal
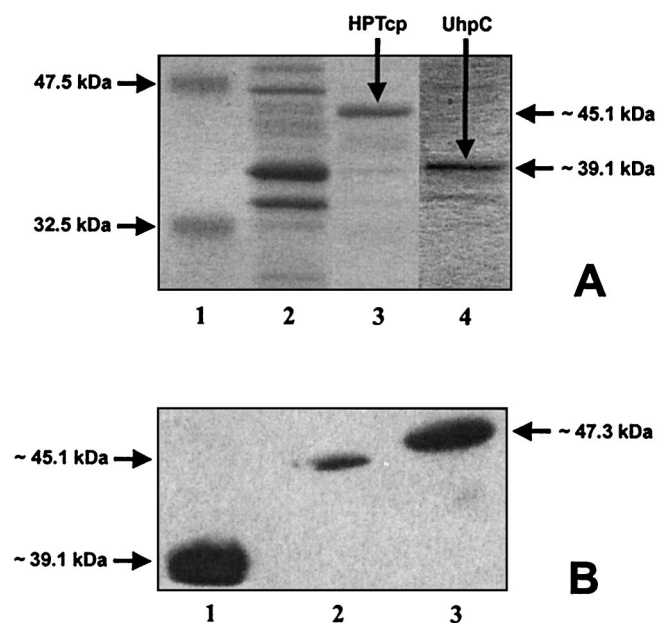
FIG. 3. Purification of histidine-tagged transport proteins and Western blot analysis. (A) Purification of His-HPTcp and His-UhpC. *E. coli* C43 cells harboring the plasmids *uhpC*/pMA618 or *hptcp*/pMA618 were induced with IPTG. The histidine-tagged proteins were enriched by metal affinity chromatography (details are given in Materials and Methods). Lane 1, marker proteins (NEB standard); lane 2, crude extract of the membrane protein fraction of His-HPTcp; lane 3, elution of His-HPTcp at an imidazole concentration of 100 mM; lane 4, elution of His-UhpC at an imidazole concentration of 100 mM. No proteins extracted from control cells (pET16b) were detectable in the elution fraction (data not shown). (B) Western blot analysis of membrane protein fractions of IPTG-induced *E. coli* BL21 cells (*uhpT*::Tn*1000*) harboring plasmid *uhpC*/pET16b, *hptcp*/pET16b, or *uhpT*/pET16b. Equal amounts of total protein were used. Immunoblotting was carried out with a histidine tag-specific antiserum (details are given in Materials and Methods). Lane 1, membrane protein fraction of His-UhpC; lane 2, membrane protein fraction of His-HPTcp; lane 3, membrane protein fraction of His-UhpT.

Glc6P transport rates were 38 nmol/mg of *E. coli* protein per h for His-UhpC (Fig. 1B), 200 nmol/mg of *E. coli* protein per h for His-HPTcp (Fig. 2B), and 2,800 nmol/mg of *E. coli* protein per h for His-UhpT (data not shown). From these data we calculated relative specific activities (maximal rate of Glc6P transport/percentage of transport protein in the *E. coli* membrane) of 0.4 for His-UhpC, 21 for His-HPTcp, and 76 for His-UhpT.

Substrate specificity of His-UhpC and His-HPTcp. It is well established that UhpT not only uses Glc6P as a substrate but also P_i and some organophosphates with widely differing apparent affinities (e.g., reference 5). To analyze and compare the substrate specificities of the sensor His-UhpC, the *E. coli* hexose phosphate transporter His-UhpT, and the chlamydial transporter His-HPTcp, we expressed the corresponding structural genes in *E. coli* (uhpT::Tn*1000*). Uptake experiments were carried out at Glc6P concentrations near the apparent K_m values (for His-UhpT at 30 μM, for His-UhpC at 25 μM, and for His-HPTcp at 100 μM). The indicated effectors were present at 20-fold above the given Glc6P concentration.

Fructose 6-phosphate (Fru6P) inhibited Glc6P uptake by

TABLE 1. Effects of various phosphorylated metabolites on [^{14}C]-Glc6P transport activity by His-UhpC, His-UhpT, or His-HPTcp[a]

Effector	Mean rate of Glc6P transport (%) ± SD		
	His-UhpC	His-UhpT	His-HPTcp
None	100	100	100
Fru6P	77 ± 5.3	9 ± 1.7	93 ± 1.4
Galactose 6-phosphate	74 ± 3.3	88 ± 1.2	62 ± 5.5
Glucosamine 6-phosphate	66 ± 3.2	38 ± 4.5	77 ± 3.5
Mannose 6-phosphate	71 ± 2.6	16 ± 2.7	84 ± 1.3
Glc1P	63 ± 4.8	39 ± 3.2	99 ± 0.7
Erythrose 4-phosphate	67 ± 2.6	95 ± 1.7	58 ± 7.0
Glycerol 3-phosphate	115 ± 0.9	91 ± 3.0	206 ± 12.7
3-Phosphoglyceric acid	98 ± 1.5	98 ± 1.8	186 ± 11.0
Phosphoenolpyruvate	105 ± 2.6	95 ± 1.1	239 ± 7.1

[a] *E. coli* cells were incubated for 1 min at a concentration of 25 μM (UhpC), 30 μM (UhpT), or 100 μM [^{14}C]Glc6P (HPTcp). Effectors were present at a 20-fold excess. The data represent the mean of three independent measurements.

His-UhpT most efficiently, reducing the uptake to ca. 9% of the control rate (Table 1). In marked contrast to this, Fru6P only modestly inhibited Glc6P uptake catalyzed by His-UhpC to 77% of the control rate and His-HPTcp to only 93% of the control rate (Table 1). Galactose 6-phosphate was a weak inhibitor in all cases (62 to 88% of the control rate). Glucosamine 6-phosphate reduced both His-UhpC and His-HPTcp activity to ca. two-thirds of the control rate, whereas Glc6P uptake by His-UhpT was reduced to ca. one-third of the residual activity (Table 1). Mannose 6-phosphate moderately affected His-UhpC and His-HPTcp activity (71 and 84% of the control rate, respectively) but strongly reduced the rate of Glc6P uptake mediated by His-UhpT (16% of the control rate; Table 1). Glc1P did not significantly affect the chlamydial transporter His-HPTcp but reduced the activity of His-UhpC protein to two-thirds and the activity of His-UhpT to one-third of the control rate (Table 1). Erythrose 4-phosphate, an intermediate of the oxidative pentose phosphate pathway, hardly affected His-UhpT activity, whereas Glc6P transport by His-UhpC and His-HPTcp was reduced to 67 and 58% of the control rate, respectively (Table 1). Remarkably, all three tested C_3-organophosphates (glycerol 3-phosphate, 3-phosphoglyceric acid, and phosphoenolpyruvate) stimulated His-HPTcp activity up to 2.4-fold but hardly affected the two *E. coli* proteins (Table 1).

Effect of P_i on Glc6P uptake by His-UhpT, His-UhpC, and His-HPTcp. UhpT-mediated Glc6P uptake into *E. coli* is classified as a P_i-linked antiporter system (22). Therefore, both substrates, Glc6P and Pi, compete for access to the same binding site of the transport protein. To define the putative competition between these compounds at the substrate binding site of His-UhpC and His-HPTcp, we analyzed the effect of rising P_i concentrations on Glc6P import. At a Glc6P concentration of 25 μM, external P_i concentrations of 2.5, 10, and 25 mM inhibited His-UhpT-catalyzed Glc6P by 7, 40, and 50%, respectively (Fig. 4). The inhibitory effect of P_i on His-UhpC-mediated Glc6P transport was remarkably stronger, with inhibitions of 50, 80, and 90% at the same P_i concentrations (Fig. 4). In contrast to the *E. coli* proteins the chlamydial transporter His-HPTcp appeared nearly unaffected by exogenous P_i (Fig. 4). In fact, at low external P_i concentrations (2.5 and 10 mM)
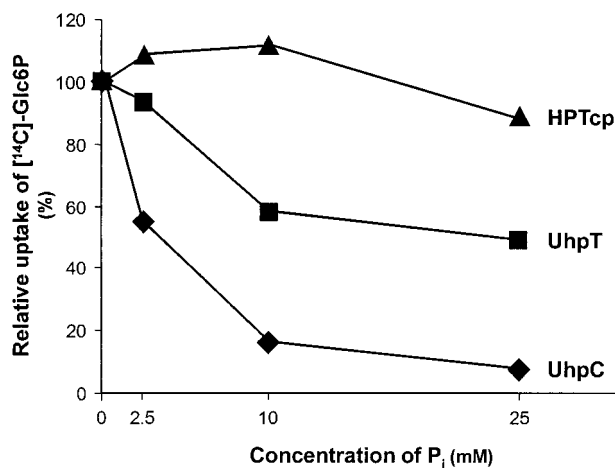
FIG. 4. Effect of P_i on Glc6P transport mediated by His-HPTcp, His-UhpC, or His-UhpT. *E. coli* cells (*uhpT*::Tn*1000*) harboring plasmids *uhpC*/pET16b (▲), *hptcp*/pET16b (◆), or *uhpT*/pET16b (■) were incubated for 1 min at a concentration of 25 μM [^{14}C]Glc6P.

the rate of Glc6P uptake was slightly increased and at 25 mM P_i an inhibition of only 8% was detected (Fig. 4). We estimated the inhibitory constant (K_i) for P_i as 4 mM for the His-UhpT protein. This value is in accordance with previously reported data (7). P_i also acts competitively on His-UhpC-mediated Glc6P import (K_i = 2.5 mM; Fig. 5). In marked contrast, rising concentrations of external P_i did not decrease the apparent substrate affinity of His-HPTcp but rather slightly increased the substrate affinity (Fig. 4 and 5C).

Antiporter properties of His-UhpC and His-HPTcp. Although all bacterial Glc6P transport systems are thought to be P_i-linked antiporters (2, 16), this has never been analyzed for the chlamydial transporter HPTcp or for the *E. coli* sensor UhpC. Therefore, we grew the *E. coli* cells in M63 medium which contains 100 mM Pi. Thus, the *E. coli* P_i uptake systems are nearly absent, and any rapid observed P_i transport should be for the most part mediated by the Glc6P antiporters (22). Both P_i uptake (100 μM $^{32}P_i$) in *E. coli* cells expressing His-UhpT, His-UhpC, or His-HPTcp and the displacement of this radiolabeled P_i with the following addition of 10 mM unlabeled P_i were measured (22).

In the case of *E. coli* cells harboring just the plasmid pET16b there was a lower level of P_i uptake than in cells expressing Glc6P transport. The addition of unlabeled P_i did not substantially affect the level of intracellular radiolabel (Fig. 6A). In contrast, cells harboring *uhpT*/pET16b released more than 80% of the radiolabel within 13 min (Fig. 6A) as expected from the work of others (22). Like His-UhpT, *E. coli* cells expressing His-UhpC or His-HPTcp rapidly released internal radiolabel after the addition of 10 mM unlabeled P_i (Fig. 6A). Furthermore, in similar experiments we demonstrated that both unlabeled Glc6P and erythrose 4-phosphate (a putative but unexpected substrate based on Table 1) could affect the release of radiolabel from cells expressing His-HPTcp that had been loaded with radioactively labeled P_i (Fig. 6B). Based on these experiments we suggest that all three Glc6P transport proteins analyzed here exhibit a P_i-Glc6P antiport mode of transport. A problem remains of how to reconcile the lack of inhibition of
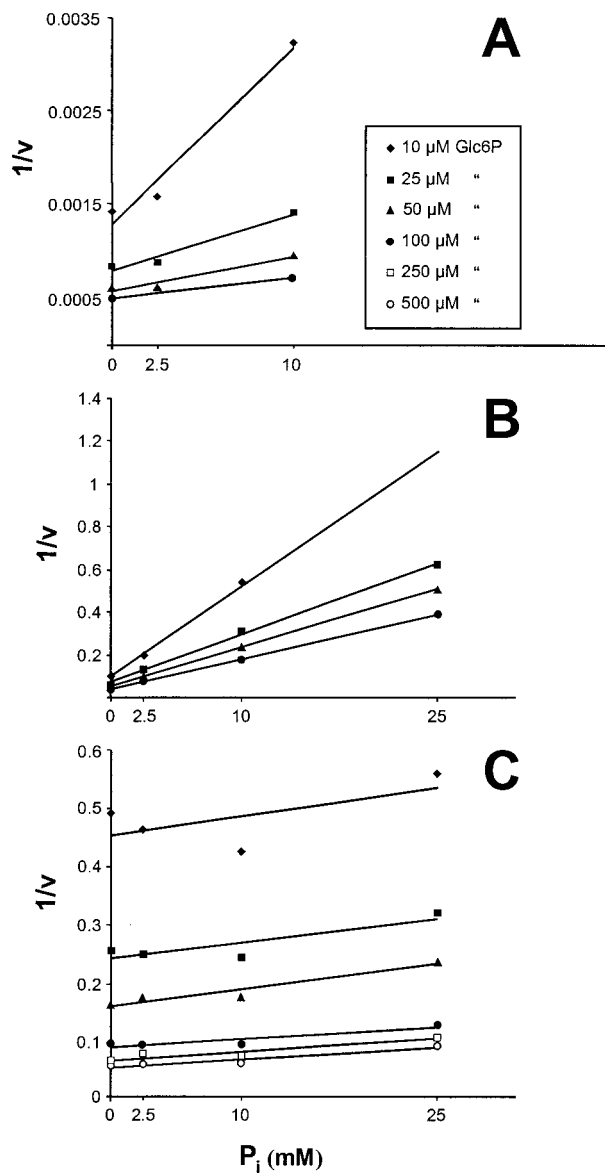

FIG. 5. Dixon plot analysis of the P_i effect on Glc6P transport. (A) Transport catalyzed by His-UhpT; (B) transport catalyzed by His-UhpC; (C) transport catalyzed by His-HPTcp. Uptake of [^{14}C]Glc6P into IPTG-induced *E. coli* cells (*uhpT*::Tn*1000*) harboring the corresponding plasmids was measured at different P_i concentrations. The apparent K_i values are 4 mM for His-UhpT and 2.5 mM for His-UhpC.

Glc6P transport by HPTcp (Fig. 4 and 5) with both the influx and efflux of P_i presumably mediated by this transporter (Fig. 6).

Complementation of an *E. coli uhpC*::Tn*1000* mutant by the His-UhpC or His-HPTcp protein. Since the amino acid sequences of HPTcp and UhpC share 67% similarity, it is of interest to determine whether the chlamydial transport protein is able to sense exogenous Glc6P, communicate this information to UhpB, and thus complement a *uhpC*::Tn*1000* mutant of *E. coli*. For this analysis, we used a *uhpC*::Tn*1000* mutant that contained an IPTG-induced *uhpC*/pET16b or *hptcp*/pET16b plasmid and analyzed the induction of the chromosomally en-
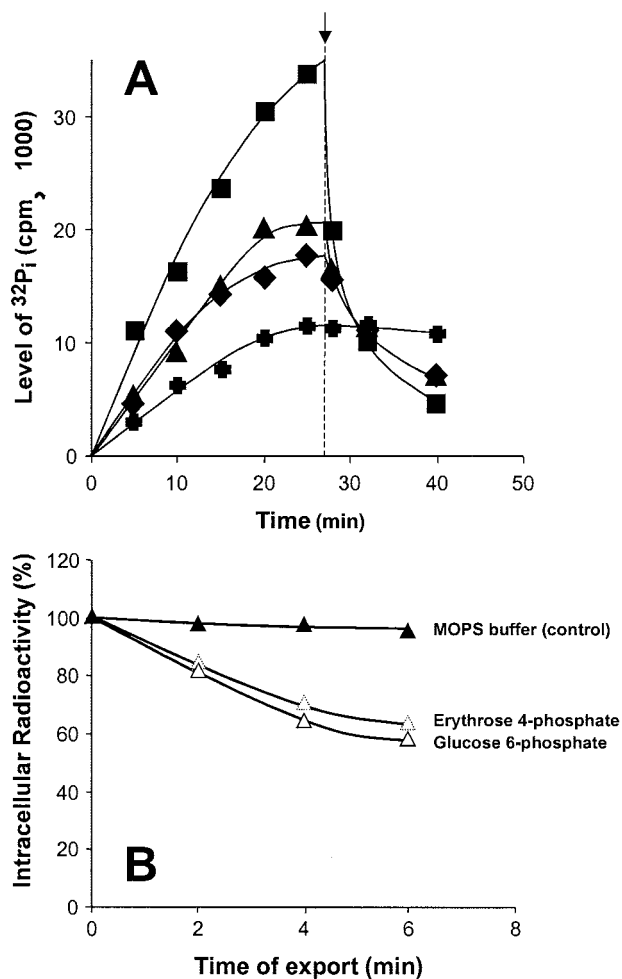
FIG. 6. Phosphate exchange across the membrane of IPTG-induced *E. coli* cells. *E. coli* cells (*uhpT*::Tn*1000*) harbored either plasmid pET16b (✚), *uhpC*/pET16b (◆), *hptcp*/pET16b (▲), or *uhpT*/pET16b (■). (A) Effect of dilution on internal P$_i$ concentration. After incubation with 100 μM ^{32}P$_i$, unlabeled P$_i$ was added to a final concentration of 10 mM (arrow). Cells were grown in M63 medium (see Materials and Methods) and washed twice with MOPS buffer medium. (B) After incubation with 100 μM ^{32}P$_i$ for 5 min and removal of external radioactivity, each suspension of IPTG-induced *E. coli* cells (*uhpT*::Tn*1000*) harboring plasmid *hptcp*/pET16b received MOPS buffer medium with or without 2 mM erythrose 4-phosphate or Glc6P.

FIG. 7. Complementation of the *uhpC*-deficient *E. coli* strain BL21 (*uhpC*::Tn*1000*) with the plasmids *uhpC*/pET16b or *hptcp*/pET16b. The corresponding suspensions were induced with IPTG and/or with 100 μM Glc6P. For determination of uptake rates the cells were incubated for 1 min with 10 μM [^{14}C]Glc6P. In column 5, 10, and 12 Fru6P (200 μM) was added during [^{14}C]Glc6P uptake. Because of the experimental design, the background activity (−IPTG, −Glc6P) was not subtracted. Columns: 1, wild-type *E. coli* BL21, −IPTG, −Glc6P; 2, wild-type *E. coli* BL21, −IPTG, +Glc6P; 3, *uhpC*-deficient *E. coli* BL21 (*uhpC*::Tn*1000*), complemented with *uhpC*/pET16b, −IPTG, −Glc6P; 4, see column 3, −IPTG, +Glc6P; 5, see column 3, −IPTG, +Glc6P, +Fru6P; 6, see column 3, +IPTG, +Glc6P; 7, *uhpC*-deficient *E. coli* BL21 (*uhpC*::Tn*1000*), complemented with *hptcp*/pET16b, −IPTG, −Glc6P; 8, see column 7, −IPTG, + Glc6P; 9, see column 7, + IPTG, −Glc6P; 10, see column 7, + IPTG, −Glc6P, +Fru6P; 11, see column 7, +IPTG, +Glc6P; 12, see column 7, +IPTG, +Glc6P, +Fru6P.

coded UhpT protein by exogenous Glc6P. The interpretation of the experiment was made difficult by the fact that IPTG-induced expression of *uhpC*/pET16b and *hptcp*/pET16b increased the transport of Glc6P independently of induction of UhpT by Glc6P (Fig. 1 and 2). However, the specific inhibition by Fru6P of Glc6P transport mediated by UhpT (but not HPTcp; Table 1) allowed us to overcome this problem.

The addition of Glc6P (100 μM) during growth of the wild-type *E. coli* cells induced the UhpT Glc6P uptake system with a rate of ca. 145 nmol/mg of *E. coli* protein per h (Fig. 7, columns 1 and 2). *E. coli* cells (*uhpC*::Tn*1000*) containing the plasmid encoding His-UhpC protein did not transport substantial amounts of Glc6P in the absence of both IPTG and Glc6P during growth (Fig. 7, column 3). Interestingly, even in the
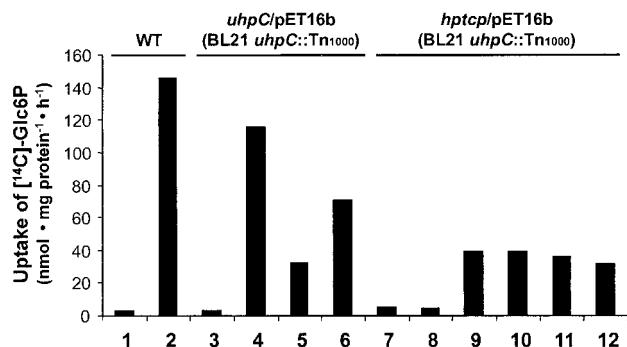
absence of IPTG the presence of Glc6P during growth of the cells resulted in a substantial capacity to transport [^{14}C]Glc6P (115 nmol/mg of *E. coli* protein per h; Fig. 7, column 4). The additional presence of Fru6P during uptake strongly inhibited Glc6P import (Fig. 7, column 5). This observation clearly showed that Glc6P uptake was mediated by UhpT (compare with the data in Table 1). The presence of both IPTG and Glc6P during growth of the cells did not lead to higher rates of Glc6P uptake than were observed without IPTG (compare columns 4 and 6 of Fig. 7). This effect might be due to an interference of large amounts of His-UhpC with other components of the *uhp* regulon.

In the absence of IPTG and Glc6P *E. coli* cells (*uhpC*::Tn*1000*) transformed with the plasmid *hptcp*/pET16b did not transport substantial amounts of Glc6P (Fig. 7, column 7). This low rate of Glc6P import was not increased by the presence of Glc6P during growth of the cells (Fig. 7, column 8). This result is in marked contrast to the observations made on the *E. coli* (*uhpC*::Tn*1000*) mutant transformed with the plasmid *uhpC*/pET16b (Fig. 7, column 4). The presence of both Glc6P and IPTG during growth of the cells resulted in a Glc6P uptake rate of ca. 39 nmol/mg of *E. coli* protein per h (Fig. 7, column 9) that was not inhibited by the addition of Fru6P (Fig. 7, column 10). This observation demonstrated that import under these conditions was solely mediated by the IPTG-induced His-HPTcp and not by the UhpT protein. In contrast to the situation in wild-type cells (Fig. 7, column 2) or in the *E. coli* *uhpC*::Tn*1000* mutant complemented with the plasmid *uhpC*/pET16b, Glc6P did not induce the chromosomal *uhpT* gene (Fig. 7, columns 11 and 12). Therefore, His-HPTcp is not able

to complement a missing UhpC protein for the induction of the *uhp* regulon.

DISCUSSION

The observation that the chlamydial transporter HPTcp exhibits a higher degree of sequence similarity to the *E. coli* Glc6P sensor UhpC than to the *E. coli* Glc6P transporter UhpT was surprising. Although the effect of several in-frame insertions into the UhpC gene on Glc6P sensing indicated that transport is not required for sensing (15), the ability of His-UhpC to transport Glc6P has now been demonstrated (Fig. 1). Maloney and coworkers identified a number of amino acids strictly required for function of UhpT. For example, the arginine residues R_{46} and R_{275} are indispensable for UhpT-mediated Glc6P transport (6). Thus, it is not surprising to find corresponding amino acid residues conserved in both UhpC and HPTcp, proteins that can function as transporters (R_{49} and R_{278} in HPTcp and R_{46} and R_{266} in UhpC). According to our data it is clear that UhpC is able to transport Glc6P (Fig. 1). However, under in vivo conditions UhpC interacts with UhpB, and such interaction might influence the transport activity of UhpC.

His-HPTcp does not complement the *uhp*C::Tn*1000* mutation in the *E. coli uhp* regulon (Fig. 7, columns 7 to 12). This observation demonstrates that a sensor function of His-HPTcp is not present even if the other elements of the *E. coli uhp* regulon are functionally present (Fig. 7, columns 3 to 6). Obviously, the structural modifications which occurred after transfer of the gene into the chlamydial cell and which are required to gain optimized transport properties (see below) led to a loss of sensing ability. In fact, the sensor function is not useful in chlamydiae because these bacteria lack all other components of the *uhp* regulon (23). Moreover, as obligate intracellular bacteria they are probably permanently exposed to a rich and homeostatically regulated metabolite medium (20). We suppose that the lower apparent substrate affinity of His-HPTcp (Fig. 2) represents one of several biochemical adaptations to the unique ecological niche chlamydial cells occupy (20). Within the host cell they are wrapped with a membrane which is permeable for a wide range of metabolites such as sugar-phosphates, various nucleoside triphosphates, and amino acids (11, 12, 19, 20, 24, 25).

In clear contrast to the *E. coli* UhpT protein the chlamydial transporter HPTcp does not transport Fru6P (Table 1). However, this feature might not represent a drawback for the pathogenic bacterial cell since phosphoglucose isomerase, catalyzing the equilibration of Glc6P and Fru6P in the host cytosol, is known to be a very active enzyme. Therefore, while the free-living *E. coli* cell does not often find both energy-rich hexose phosphates and enzymes mediating their equilibration in their external milieu, the obligately intracellular chlamydial cell can rely on the presence of both types of molecules (metabolites and enzymes) in their environment. In addition, His-HPTcp is unable to transport mannose 6-phosphate (Table 1). This feature is in accordance with the absence of genes encoding mannose 6-phosphate isomerases in the chlamydial genome (23). Without this enzyme mannose 6-phosphate cannot be used to fuel bacterial metabolism. In contrast to His-UhpT, His-HPTcp is able to transport erythrose 4-phosphate (Table 1; Fig. 6B). The biological significance of such transport remains unclear since the chlamydial genome contains the genes to encode all of the enzymes required to synthesize erythrose 4-phosphate via the oxidative pentose phosphate pathway.

Although Glc6P transport mediated by His-UhpT and His-UhpC is competitively inhibited by exogenous P_i (Fig. 5A and B), Glc6P uptake into *E. coli* cells expressing the chlamydial transport protein His-HPTcp is not (Fig. 5C). Under in vivo conditions an absence of P_i inhibition on Glc6P import might represent an advantage for the pathogenic bacterium. It has been demonstrated that primary metabolism in chlamydial cells depends on Glc6P uptake (13). Assuming that in the late phase of host cell infection an inhibition of the eukaryotic energy metabolism occurs, a corresponding increase of P_i (less ATP and phosphorylated intermediates) will still allow uptake of the required Glc6P (Fig. 5C), thus maintaining of bacterial metabolism under unfavourable conditions. However, the exact function of P_i on the His-HPTcp protein seems to be much more complex because this lack of inhibition by P_i of HPTcp activity must be reconciled with the readily observed influx and efflux of P_i presumably mediated by this transporter (Fig. 6). A more detailed analysis requires the establishing of a proteoliposome system harboring the heterologously synthesized and enriched HPTcp protein.

Another clear difference in the two *E. coli* proteins is the stimulatory effect of the C_3-organophosphates PGA, PEP, and glycerol 3-phosphate on Glc6P transport catalyzed by His-HPTcp (Table 1). The specificity of this effect is indicated by the observation that these compounds do not affect the His-UhpT or His-UhpC proteins (Table 1). It may be that His-HPTcp possesses domains on its periplasmic side, allowing it to bind C_3-organophosphates. Recently, it has been shown that mutants of UhpT lacking the intrahelical salt bridge between amino acid residues D_{388} and K_{391} now transport phosphoenolpyruvate but have lost the ability to transport Glc6P (9). Neither UhpC nor HPTcp contain charged amino acids at the corresponding positions (UhpC, T_{383} and V_{386}; HPTcp, S_{396} and T_{399}), showing that this intrahelical salt bridge does not determine substrate specificity in these two proteins. However, it will be interesting to introduce a corresponding salt bridge in UhpC and HPTcp to determine whether we might be able to alter their specificity or specific activity.

The similarity of the amino acid sequences of HPTcp and UhpC indicates that *hptcp* derives from a horizontal gene transfer between a bacterial species harboring a *uhp* regulon and a relative of recent *Chlamydia*. If we compare the biochemical features of His-UhpC and His-HPTcp in more detail further evidences for a common evolutionary ancestor are raised. Among the six phosphorylated intermediates inhibiting Glc6P import catalyzed by all three types of proteins (His-UhpT, His-UhpC, and His-HPTcp) four (Fru6P, glucosamine 6-phosphate, mannose 6-phosphate, and erythrose 4-phosphate) act very similarly on His-UhpC and His-HPTcp but totally differently on His-UhpT (Table 1). The observation that phosphorylated intermediates other than Glc6P hardly affect UhpC (Table 1) is in full accordance with previous observations on the sensor function of this protein (15). Because His-UhpC is able to catalyze Glc6P import (Fig. 1; Table 1), there is no biochemical constraint to exclude the occurrence of such a horizontal transfer to confer Glc6P import. Remark-

ably, the membranes from the human endoplasmic reticulum (brain isoform) also contain a Glc6P transport protein that exhibits a higher degree of identity to UhpC (29.3%) than to UhpT (21.4%) (8, 18). Interestingly, the chlamydial hexose phosphate transporters exhibit an even higher degree of similarity to the human endoplasmic reticulum homologs (~33%) (18), raising the question about the evolutionary relationship between the bacterial and the human types of these carrier systems. In this context, it is worthwhile to mention that the extremely reduced chlamydial genome contains at least 35 genes of eukaryotic origin (23). Obviously, it will be interesting for evolutionary biologists to analyze the phylogenetic origin of the *hptcp* gene (either from other bacteria or from a eukaryotic origin) in detail.

REFERENCES

1. **Alexeyev, M. F., and H. H. Winkler.** 1999. Membrane topology of the *Rickettsia prowazekii* ATP/ADP translocase revealed by novel dual *pho-lac* reporters. J. Mol. Biol. **285:**1503–1513.
2. **Ambudkar, S. V., and P. C. Maloney.** 1984. Characterization of phosphate: hexose 6-phosphate antiport in membrane vesicles of *Streptococcus lactis*. J. Biol. Chem. **259:**12576–12585.
3. **Arber, W.** 1958. Transduction of chromosomal genes and episomes in *E. coli*. Virology **11:**250–272.
4. **Bradford, M. M.** 1976. A rapid and sensitive method for the quantification of microgram quantities of protein utilizing the principle of protein-dye binding. Anal. Biochem. **72:**248–254.
5. **Dietz, G. W.** 1976. The hexose phosphate transport system of *Escherichia coli*. Adv. Enzymol. **44:**237–259.
6. **Fann, M., A. H. Davies, A. Varadhachary, T. Kuroda, C. Sevier, T. Tsuchiya, and P. C. Maloney.** 1998. Identification of two essential arginine residues in UhpT, the sugar phosphate antiporter of *Escherichia coli*. J. Membr. Biol. **164:**187–195.
7. **Fann, M. C., and P. C. Maloney.** 1998. Functional symmetry of UhpT, the sugar phosphate transporter of *Escherichia coli*. J. Biol. Chem. **273:**33735–33740.
8. **Gerin, I., M. Veiga-da-Cunha, Y. Achouri, J.-F. Collet, and E. Van Schaftingen.** 1997. Sequence of a putative glucose 6-phosphate translocase, mutated in glycogen storage disease type Ib. FEBS Lett. **419:**235–238.
9. **Hall, J. A., and P. C. Maloney.** 2001. Transmembrane segment 11 of UhpT, the sugar phosphate carrier of *Escherichia coli*, is an alpha-helix that carries determinants of substrate selectivity. J. Biol. Chem. **276:**25107–25113.
10. **Hall, J. A., M. Fann, and P. C. Maloney.** 1999. Altered substrate selectivity in a mutant of an intrahelical salt bridge in UhpT, the sugar phosphate carrier of *Escherichia coli*. J. Bacteriol. **274:**6148–6153.
11. **Hatch, T. P.** 1975. Utilization of L-cell nucleoside triphosphates by *Chlamydia psittaci* for ribonucleic acid synthesis. J. Bacteriol. **122:**393–400.
12. **Hatch, T. P., E. Al-Hossainy, and J. A. Silverman.** 1982. Adenine nucleotide and lysine transport in *Chlamydia psittaci*. J. Bacteriol. **150:**662–670.
13. **Iliffe-Lee, E. R., and G. McClarty.** 2000. Regulation of carbon metabolism in *Chlamydia trachomatis*. Mol. Microbiol. **38:**20–30.
14. **Island, M. D., B. Y. Wei, and J. J. Kadner.** 1992. Structure and function of the *uhp* genes for the sugar phosphate transport system in *E. coli* and *Salmonella typhimurium*. J. Bacteriol. **174:**2754–2762.
15. **Kadner, R. J., M. D. Island, J. L. Dahl, and C. A. Webber.** 1994. A transmembrane signalling complex controls transcription of the Uhp sugar phosphate transport system. Res. Microbiol. **145:**381–387.
16. **Maloney, P. C., S. V. Ambudkar, J. Thomas, and L. Schiller.** 1984. Phosphate/hexose 6-phosphate antiport in *Streptococcus lactis*. J. Bacteriol. **158:** 238–245.
17. **Marger, M. D., and M. H. Saier.** 1993. A major superfamily of transmembrane facilitators that catalyse uniport, symport and antiport. Trends Biol. Sci. **18:**13–20.
18. **Méchin, M.-C., and G. van de Werve.** 2000. Glucose-6-phosphate transporter and receptor functions of the glucose 6-phosphatase system analyzed from a consensus defined by multiple alignments. Proteins Struct. Funct. Genet. **41:**164–172.
19. **Moulder, J. M.** 1962. The Biochemistry of intracellular parasitism. The University of Chicago Press, Chicago, Ill.
20. **Moulder, J. M.** 1991. Interaction of chlamydiae and host cells in vitro. Microbiol. Rev. **55:**143–190.
21. **Sambrook, J., E. F. Fritsch, and T. Maniatis.** 1989. Molecular cloning: a laboratory manual, 2nd ed. Cold Spring Harbor Laboratory, New York, N.Y.
22. **Sonna, L. A., S. V. Ambudkar, and P. C. Maloney.** 1988. The mechanism of glucose 6-phosphate transport by *Escherichia coli*. J. Biol. Chem. **263:**6625–6630.
23. **Stephens, R. S., S. Kalman, C. Lammel, J. Fan, R. Marathe, L. Aravind, W. Mitchell, L. Olinger, R. L. Tatusol, Q. Zhao, E. V. Koonin, and R. W. Davis.** 1998. Genome sequence of an obligate intracellular pathogen of humans: *Chlamydia trachomatis*. Science **282:**754–759.
24. **Tipples, G., and G. McClarty.** 1993. The obligate intracellular bacterium *Chlamydia trachomatis* is auxotrophic for three of the four ribonucleoside triphosphates. Mol. Microbiol. **8:**1105–1114.
25. **Tjaden, J., M. van der Laan, C. Schwöppe, T. Möhlmann, H. H. Winkler, and H. E. Neuhaus.** 1999. Two nucleotide transport proteins in *Chlamydia trachomatis*. One for net nucleoside triphosphate uptake and the other for the transport of energy. J. Bacteriol. **181:**1196–1202.
26. **Winkler, H. H.** 1973. Distribution of an inducible hexose-phosphate transport system amongst various bacteria. J. Bacteriol. **116:**1079–1081.
27. **Wright, J. S., III, and R. J. Kadner.** 2001. The phosphoryl transfer domain of UhpB interacts with the response regulator UhpA. J. Bacteriol. **183:**3149–3159.